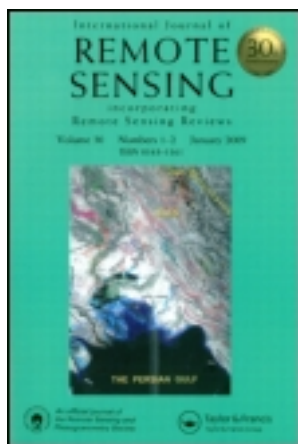


This article was downloaded by: [Samir Kamh]

On: 08 November 2011, At: 15:50

Publisher: Taylor & Francis

Informa Ltd Registered in England and Wales Registered Number: 1072954 Registered office: Mortimer House, 37-41 Mortimer Street, London W1T 3JH, UK



International Journal of Remote Sensing

Publication details, including instructions for authors and subscription information:

<http://www.tandfonline.com/loi/tres20>

Evaluating urban land cover change in the Hurghada area, Egypt, by using GIS and remote sensing

Samir Kamh ^a, Mahmoud Ashmawy ^a, Adamantios Kiliass ^b & Basile Christaras ^b

^a Department of Geology, Faculty of Science, Tanta University, Tanta, 31527, Egypt

^b Department of Geology, School of Geology, Aristotle University of Thessaloniki, Thessaloniki, 54124, Greece

Available online: 08 Nov 2011

To cite this article: Samir Kamh, Mahmoud Ashmawy, Adamantios Kiliass & Basile Christaras (2012): Evaluating urban land cover change in the Hurghada area, Egypt, by using GIS and remote sensing, International Journal of Remote Sensing, 33:1, 41-68

To link to this article: <http://dx.doi.org/10.1080/01431161.2010.550331>

PLEASE SCROLL DOWN FOR ARTICLE

Full terms and conditions of use: <http://www.tandfonline.com/page/terms-and-conditions>

This article may be used for research, teaching, and private study purposes. Any substantial or systematic reproduction, redistribution, reselling, loan, sub-licensing, systematic supply, or distribution in any form to anyone is expressly forbidden.

The publisher does not give any warranty express or implied or make any representation that the contents will be complete or accurate or up to date. The accuracy of any instructions, formulae, and drug doses should be independently verified with primary sources. The publisher shall not be liable for any loss, actions, claims, proceedings, demand, or costs or damages whatsoever or howsoever caused arising directly or indirectly in connection with or arising out of the use of this material.

Evaluating urban land cover change in the Hurghada area, Egypt, by using GIS and remote sensing

SAMIR KAMH*†, MAHMOUD ASHMAWY†, ADAMANTIOS KILIAS‡
and BASILE CHRISTARAS‡

†Department of Geology, Faculty of Science, Tanta University, Tanta 31527, Egypt

‡Department of Geology, School of Geology, Aristotle University of Thessaloniki,
Thessaloniki 54124, Greece

(Received 6 December 2007; in final form 1 October 2010)

The rapid urban development in the Hurghada area since the 1980s has dramatically enhanced the potential impact of human activities. To inventory and monitor this urban development effectively, remote sensing provides a viable source of data from which updated land cover information can be extracted efficiently and cheaply. In this study, data from three satellite datasets, Landsat Thematic Mapper (Landsat 5 TM), Landsat Enhanced Thematic Mapper Plus (Landsat 7 ETM+) and Terra/Advanced Spaceborne Thermal Emission and Reflection Radiometer (ASTER), acquired during 1987, 2000 and 2005, respectively, were used to detect and evaluate Hurghada's urban expansion. Five change detection techniques were tested to detect areas of change. The techniques considered were image differencing, image ratioing, image overlay, multivariate principal component analysis (PCA) and post-classification comparison. The post-classification comparison was found to be the most accurate procedure and produced three land use/land cover (LULC) maps of the years 1987, 2000 and 2005 with overall accuracies of 87.8%, 88.9% and 92.0%, respectively. The urban expansion analysis revealed that the built-up area has expanded by ~40 km² in 18 years (1987–2005). In addition, 4.5 km² of landfill/sedimentation was added to the sea as a result of the coastal urban development and tourist activities. The booming coastal tourism and population pressure were considered to be the main factors driving this expansion, and some natural and artificial constraints constrained the physical shape of the city. The expansion is represented by urban fringe development, linear, infill and isolated models. Topography, lithology and structures were also analysed as possible factors that influenced the expansion. The understanding of the spatial and temporal dynamics of Hurghada's urban expansion is the cornerstone for formulating a view about the future urban uses and for making the best use of the limited resources that are available.

1. Introduction

From a broader perspective, urbanization is just one of the many ways in which humans are altering the land cover of the globe. Hence, this urbanization is a complicated process that is determined by the interactions of biophysical factors and

*Corresponding author. Email: skamh2002@yahoo.com

human factors in space and time at different scales (Barredo *et al.* 2003, He *et al.* 2006). Urbanization has been studied extensively in the last few decades because of the increasing interest in environmental issues. Since the Stockholm Conference on human environment (1972) and continuing now, scientists, planners and researchers have paid much more attention to the issues of land cover changes (Loveland *et al.* 1991, Dale *et al.* 1993, Romero *et al.* 1999).

Our inability to monitor land cover changes in a consistent way over the long term is a serious limitation in our capacity to understand the driving forces and processes controlling these changes (Bounfour and Lambin 1999). The process of urbanization has been characterized not only by population growth, but also by industrial expansion, increasing economic and social activities and intensified use of land resources (Karuga 1993). Furthermore, decision-makers are in constant need of current geospatial information on patterns and trends in land cover changes. Therefore, regular and up-to-date information on urban change is required for urban planning, land use management and appropriate allocation of services and infrastructure within the urban areas (Barnsley and Barr 1996).

Remote sensing has the potential to provide accurate and timely geospatial information describing changes in urban land cover (Alberti *et al.* 2004, Xiao *et al.* 2006). The importance of remote sensing was emphasized as a 'unique view' of the spatial and temporal dynamics of the processes in urban growth and land use change (Batty and Howes 2001, Herold *et al.* 2003). Satellite remote-sensing techniques have, therefore, been widely used in detecting and monitoring land cover change at various scales with useful results (e.g. Wilson *et al.* 2003, Mundia and Aniya 2005, Shalaby and Tateishi 2007). Recently, remote sensing has been used in combination with geographical information systems (GIS) and global positioning systems (GPS) to assess land cover change more effectively than by remote-sensing data only (Müller and Zeller 2002). This combination has already been proven to be useful in mapping urban areas and as a data source for the analysis and modelling of urban growth and land use/land cover (LULC) change (e.g. Grey *et al.* 2003, Herold *et al.* 2003, Wilson *et al.* 2003).

2. The study area

The study area extends approximately between latitudes 27° 03' N and 27° 25' N and longitudes 33° 35' E and 33° 55' E on the Red Sea coast of Egypt (figure 1) and it covers about 750 km². Hurghada acts as a city and tourist centre on the Red Sea coast of Egypt. It was founded in the early twentieth century, and since the 1980s it has gone from a desert area and primitive fishing village to a thriving modern city. It is the administrative capital of the Red Sea Governorate (RSG) and is served by Hurghada international airport. The Hurghada area is composed mainly of three administrative sectors: El-Gouna resort, Hurghada city and Sahl Hashish area, which have experienced an extension of 60 km along the shoreline.

Hurghada city counts 860 971 inhabitants (Central Agency for Public Mobilization and Statistics (CAPMAS) 2006) and is divided into three parts: downtown (ad-Dahhar area), which is the oldest part; the harbour area (as-Saqqalah); and el-Ahhya area which is the modern northern part of the city. El-Gouna resort was constructed in the middle of the 1990s about 20 km north of Hurghada city and spreads over an area of 11 million m² and has about 11 km beach front (Saad 1999). It lies on the alluvial fan of Wadi (Valley) Umm Dihays, over the old Graeco-Roman port called



Figure 1. Location map of the study area.

Myos Hormos (Said 1999). In addition, Sahl Hashish area is a promising area for the future expansion of Hurghada in the south.

Climatologically, Hurghada area is characterized by dry weather and clear and warm water. The average humidity is about 54% in summer and 55% in winter. The average temperature varies between 38°C and 23°C in summer and between 29°C and 7°C in winter (Mohamed 1999). Rainfall is scarce and sparse (5 mm to a maximum of 25 mm per annum), but this rate does not reflect the real influence of

running water on the coastal area, where occasional torrential floods take place and contribute huge quantities of water and sediments to the near shore area (Moufaddal 2005).

3. Objectives

The main objectives of this study are the following: to use remotely sensed data and GIS together with socio-economic data (1) to investigate the geomorphological, lithological and structural features as physical factors influencing the urban expansion; (2) to examine the scope and rate of urban expansion using change detection techniques; (3) to detect the urban expansion directions and land use conversions that have occurred in the Hurghada area; (4) to analyse the driving forces and factors influencing the urban expansion; (5) to examine the changes in the position of the coastline linked to the urban expansion; and finally (6) to formulate a future view of Hurghada's urban expansion.

4. General considerations

Geomorphological, lithological and structural features have major contributions in evaluating the locations and growth directions of urban areas and in potential site suitability.

Geomorphologically, the study area can be broadly divided from east to west into three geomorphological units: the coastal plain, the pediment and the mountainous terrain. The coastal plain (where Hurghada city and tourist facilities are constructed) is relatively wide and covered by Pleistocene reefal limestone, gravels and sands and recent sediments. The pediment represents the interference zone between the coastal plain and the mountainous terrain and forms an inclined plain. It has a good potential for urban expansion of Hurghada in the future, but it should be under suitable management scenarios. Mountainous terrain is composed of Precambrian basement rocks (igneous and metamorphic), which are northwesterly trending and highly dissected by faults, dikes and drainage lines. It contains the second highest peak in Egypt, Gabal (mountain) Shayeb al-Banat (+2187 m), which offers a stark contrast to the coastal plain at the edge of the Red Sea.

Lithologically, the study area is covered by Precambrian basement rocks and Tertiary–Quaternary sedimentary rocks and sediments. The basement rocks include metavolcanics, metagabbros, older granites, Dokhan volcanics, Hammamat sediments and younger granites arranged from oldest to youngest (Egyptian Geological Survey and Mining Authority (EGSMA) 2005). The sedimentary rocks range in age from Miocene to Recent and form discontinuous exposures in the study area. They have regional eastward dip with dip angles ranging from 35° near basement rocks contact to nearly horizontal near the shoreline (Said 1990). These rocks are composed mainly of argillaceous limestones, conglomerates, shale, mudstone and a considerable unit of evaporites (Darwish and El-Azabi 1993).

Structurally, the syn-rift sedimentary rocks of the study area are located in the southern part of the Gulf of Suez rift, which is controlled by normal faults and tilted blocks (Colleta *et al.* 1988). The fault pattern of this area consists of two major sets: (1) the main Clysmic fault trend (N 40°–30° W) containing normal faults parallel to the rift axis that were created during Neogene time in a pure extensional regime (Colleta *et al.* 1988) and (2) transfer faults with NNE, WNW and ENE trends (Patton *et al.* 1994). The two major sets are inherited from the pre-rift basement tectonics

(Montenat *et al.* 1988) and their reactivation and hard linkage produced a zigzag fault pattern at the rift border and intra-rift system (Younes and McClay 2002).

From the viewpoint of seismic hazard, the study area lies in the southern part of the Gulf of Suez, which is one of the most seismically active zones in Egypt (Hussein *et al.* 2006). Hussein *et al.* (2006) added that the present area recorded an earthquake of magnitude about 7.2 M_s on 31 March 1969 and a number of epicentres are clustered under Shadwan Island to the northeast of Hurghada region.

5. Satellite images and reference data

The effectiveness of information on urban changes for planning and management decision-making, particularly in developing countries, depends upon the availability of useful data (Weber and Puissant 2003). To achieve the objectives of this study, Landsat Thematic Mapper (Landsat 5 TM) data acquired on 14 August 1987, Landsat Enhanced Thematic Mapper Plus (Landsat 7 ETM+) data acquired on 10 September 2000 and Advanced Spaceborne Thermal Emission and Reflection Radiometer (ASTER) data acquired on 27 November 2005 were selected as the basis for image analysis and land cover classification. Data from the three images cover a time period of 18 years. The TM-1987 data were used as the reference situation and ASTER-2005 data were used as the up-to-date situation of the Hurghada area. The datasets are cloud-free scenes acquired, relatively, during the late summer or early fall time of the year.

Reference data for ground control points (GCPs) and accuracy assessment including aerial photographs (scale 1:40 000), photomosaics (scale 1:50 000), topographic maps (scale 1:50 000), a land use map (scale 1:15 000) and geologic maps at different scales (1:500 000, 1:250 000, 1:100 000), as well as demographic data, were used in this study. The data processing and manipulation were conducted using ENVI (V. 4.5, ITT Visual Information Solutions Group (ITT VIS), formerly known as Research Systems Inc. (RSI), Boulder, CO, USA) and ArcGIS (V. 9.3, Environmental Systems Research Institute (ESRI), Redlands, CA, USA) softwares. In addition, two field surveys were carried out in September 2004 and August 2006. During these surveys, ground control, training and ground truth points were collected by using Magellan GPS-530.

6. Methodology

Digital change detection is the process of determining and/or describing changes in land cover and land use properties based on co-registered multi-temporal remote-sensing data (Shalaby and Tateishi 2007). The change detection methods were presented and reviewed by Chen (2002). They are grouped into two main approaches: (1) detecting binary change/no change information and (2) detecting the 'from-to' change map (Lu *et al.* 2004).

In the first approach, several procedures were developed, such as image differencing, image ratioing, image overlay and principal component analysis (PCA). The advantages of these procedures include the relatively rapid means of displaying areas of change and being direct and straightforward (Moufaddal 2005). Disadvantages include outlining the area of changes without giving any figures or estimates on the type and volume of the change (Mundia and Aniya 2005). The second approach includes the post-classification comparisons. This approach requires very good accuracy in the classification because the accuracy of the change map is the product of the accuracies of the individual classifications (Singh 1989). The processing procedures

which are adopted in this study are summarized in figure 2 and will be discussed in the following sections.

6.1 *Satellite image preprocessing*

Among the various aspects of image preprocessing for land cover change detection, there are two outstanding requirements: multi-temporal image registration and radiometric and atmospheric correction (Coppin and Bauer 1996, Lu *et al.* 2004, Paolini *et al.* 2006).

6.1.1 Geometric correction. The major task of the image preprocessing is the geometric registration (Ji *et al.* 2001). The importance of accurate spatial registration of multi-temporal images is obvious because largely spurious results of change detection will be produced if there is misregistration (Stow and Chen 2002).

In this study, Landsat 7 ETM+ data were co-registered to the topographic base maps at a scale of 1:50 000 (i.e. image-to-map registration) using the Universal Transverse Mercator (UTM) Projection Zone 36 North with a World Geodetic System (WGS) 84 datum. Image-to-map registration was done using 25 GCPs at a root mean square (RMS) error of less than 0.7 pixels. These points should be enough and well distributed around the edges of the image to be corrected with a scattering of them over the body of the image (Richards 1993). Landsat 5 TM and ASTER images were co-registered to the corrected Landsat 7 ETM+ at RMS errors of ~ 0.3 pixels and < 0.4 pixels, respectively. The first-order polynomial transformation and the nearest neighbour method of sampling were used to maintain the original pixel brightness values and to resample the pixels at a spacing of 30 m in both directions. A digital elevation model (DEM) of the study area with 20×20 m grid was used to evaluate the registration process.

6.1.2 Radiometric and atmospheric corrections. Radiometric consistency among ground targets in multi-temporal imagery is difficult to maintain due to changes in sensor characteristics, atmospheric condition, solar angle and sensor view angle (Du *et al.* 2002, Chen *et al.* 2005). Therefore, radiometric corrections are often performed on multi-temporal imagery to reduce any or all of the above influences and increase sensitivity to landscape change (e.g. Chavez 1996, Song *et al.* 2001, Paolini *et al.* 2006, Zhang *et al.* 2008). Since the launch of the first Landsat in 1972, numerous methods have been proposed to calibrate and normalize the satellite data (Olthof *et al.* 2005). These radiometric methods can be grouped into two major categories: absolute correction and relative correction (Thome *et al.* 1997, Song *et al.* 2001, Du *et al.* 2002).

The three datasets (Landsat TM, ETM+ and ASTER) that are used in this study were converted from raw digital numbers (DNs) to at-sensor radiance using ENVI image preprocessing utilities and based on their respective published calibration parameters given in Chander *et al.* (2004, 2007) for Landsat 5 TM sensor, Irish (2000) for Landsat 7 ETM+ sensor and Abrams and Hook (1998) for ASTER sensor.

In the absence of the detailed data on atmospheric conditions, a dark object subtraction (DOS) approach (Song *et al.* 2001) was used to convert at-sensor radiance to surface reflectance, which involves the correction of effects caused by both solar angle and atmosphere (Lu *et al.* 2002). DOS is perhaps the simplest yet most widely used image-based absolute atmospheric correction approach for classification and change

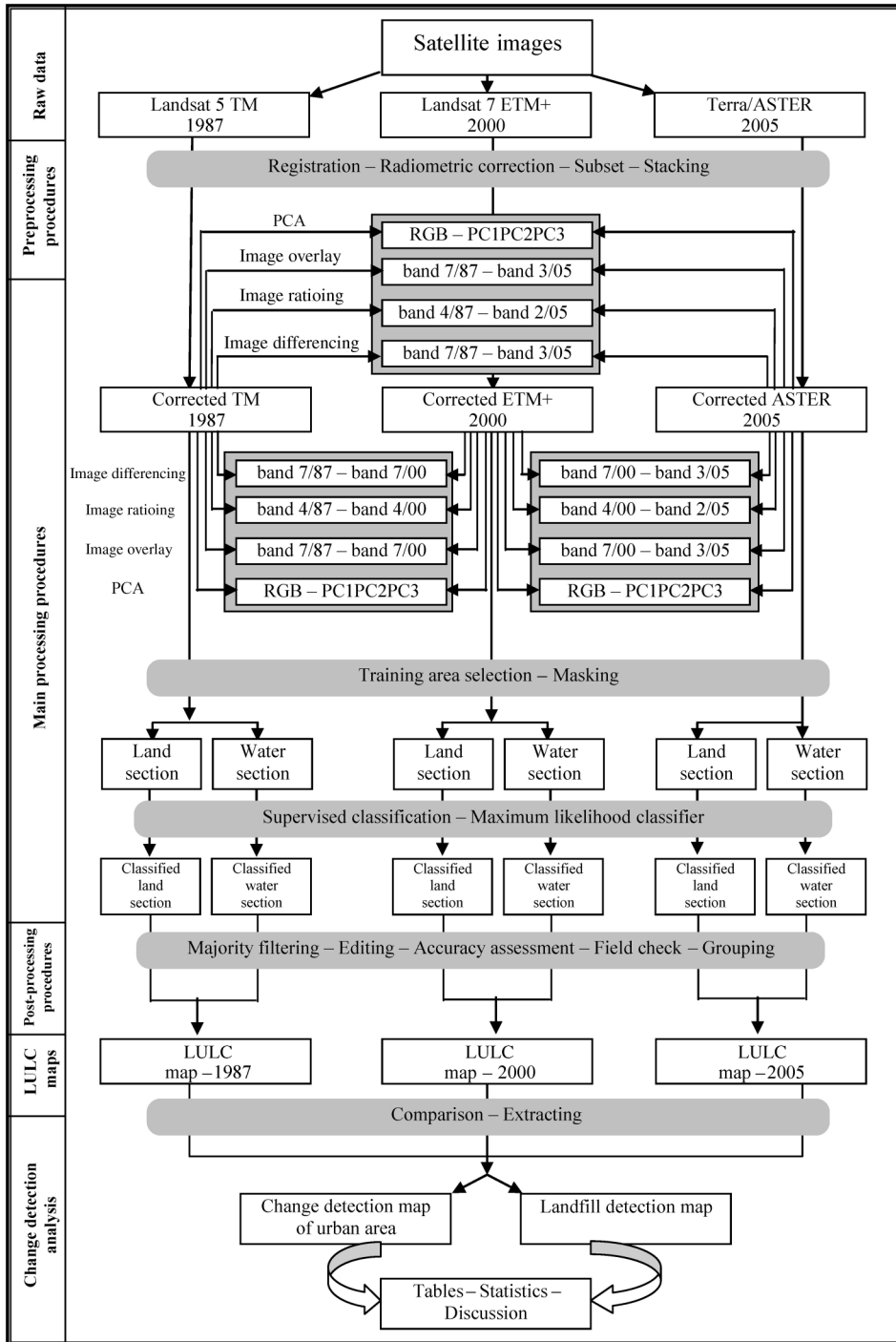


Figure 2. Flow diagram showing the adopted methodology and data processing of remote-sensing datasets.

Note: PCA, principal component analysis; LULC, land use/land cover; TM, Thematic Mapper; ETM+, Enhanced Thematic Mapper Plus; ASTER, Advanced Spaceborne Thermal Emission and Reflection Radiometer.

detection applications (Song *et al.* 2001, Paolini *et al.* 2006). A group of pixels of the deep sea water was chosen as a dark object in each spectral band of the three datasets (Landsat TM, ETM+ and ASTER) of this study. Then, the representative values of these pixels were subtracted from all the pixels of each corresponding band in each scene.

To assure that the three images used in this study appear as if they were acquired under the very same conditions, a relative radiometric normalization technique was performed. Landsat 7 ETM+ image was used as a reference image to which the different bands of the Landsat 5 TM and ASTER (bands 1, 2 and 3N) images were adjusted. This image was selected because of its central location in the time series (Schroeder *et al.* 2006). Twelve pseudo-invariant features (PIFs) were selected, seven over dark sea water and the others over bright sands. Normalization was accomplished on a band-by-band basis using these 12 PIFs. A linear relationship was assumed between the different bands of the reference and target images across time over the 12 PIFs, with coefficients of determination (R^2) ranging between 0.91 and 0.98.

The final preprocessing step was a feature selection to reduce the size of the datasets (Mather 1999). Accordingly, three subset scenes of 1111 by 1388 pixels covering the study area were extracted from the full scenes.

6.2 Change detection approaches

6.2.1 Image differencing. Image differencing is the most widely used change detection technique (Moufaddal 2005). The process simply subtracts one digital image pixel by pixel from another, to generate a third image composed of the numerical differences between pairs of pixels (Sunar 1998, Dewidar 2002, Moufaddal 2005). The difference in the areas of no change will be very small, and areas of change will reveal larger positive or negative values (Lillesand and Kiefer 2000).

In this study, an image differencing routine was carried out using ENVI software to extract a difference map representing the differences between the initial state and final state images. Many tests were carried out on the different bands of the three images (TM, ETM+ and ASTER) and these tests showed that difference maps of band 7 of TM and band 3N of ASTER displayed the urban growth and shoreline shifts (figure 3(a)). The resulting map is colour coded with 11 classes to indicate the magnitude of the changes between the two images. Positive changes are displayed in shades of red (e.g. landfill areas and coral reefs), while negative changes are displayed in shades of blue (e.g. built-up, airport and man-made lakes).

6.2.2 Image ratioing. Image ratioing is a powerful technique for extracting spectral information from multi-spectral imagery (Dewidar and Frihy 2003). When one spectral band is divided by another, an image with relative intensities will be produced (Environment for Visualizing Images (ENVI) 2004). Ratios for areas of no change tend towards 1 and areas of change will have higher or lower ratio values (Lillesand and Kiefer 2000). Dewidar (2002) successfully used the ratio of Landsat TM band 4 of 1984 and 1997 data to detect landfill along the coastline of the present study area between 1984 and 1997.

In this study, the ratio of band 4 of TM and band 2 of ASTER gave the best results and highlighted the changes in urban growth, vegetation and seagrass (figure 3(b)). The resulting image was in greyscale but subjected to an ENVI colour scheme to show the changes in the urban area over an 18-year period as a red colour (figure 3(b)).

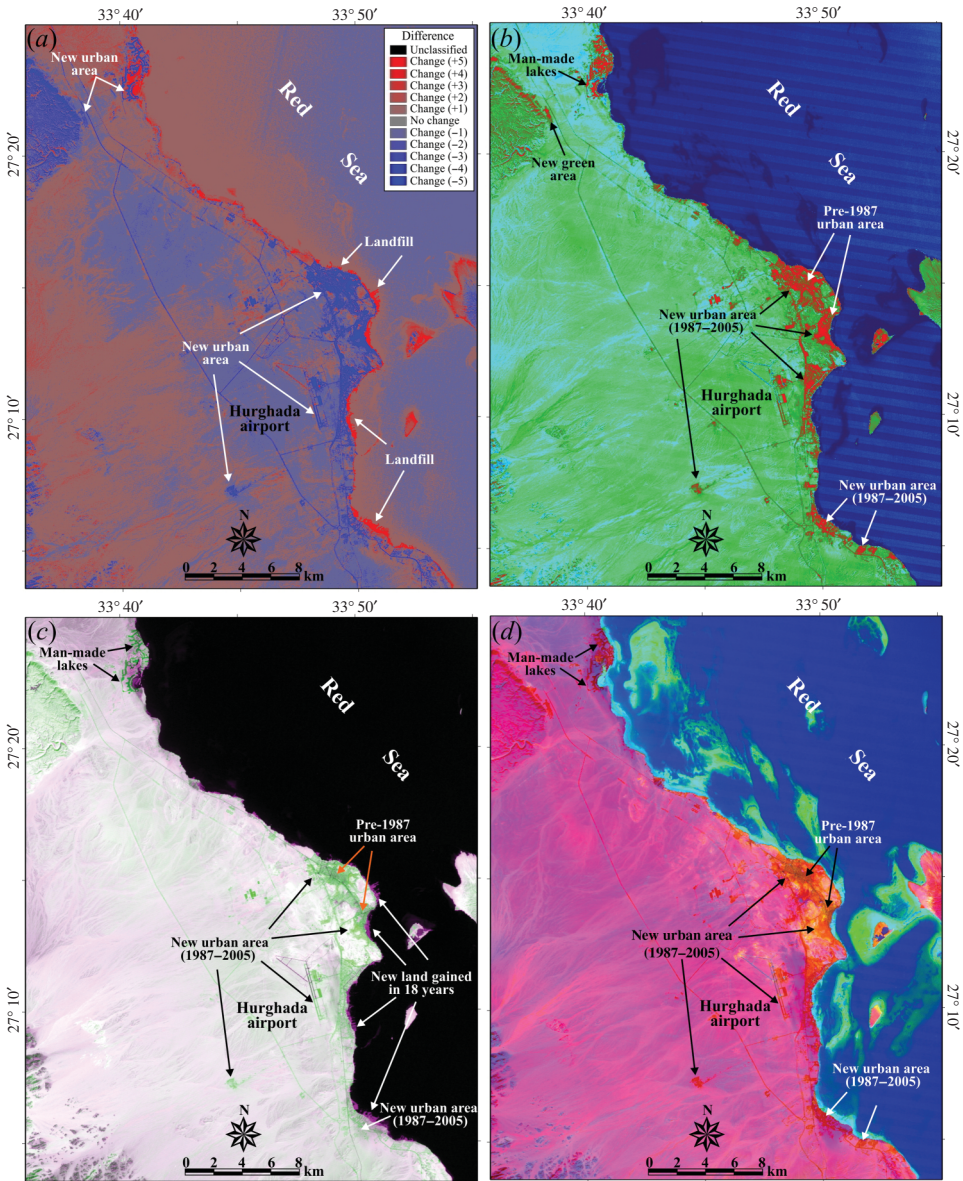


Figure 3. (a) Difference map between band 7 of Thematic Mapper (TM) and band 3N of Advanced Spaceborne Thermal Emission and Reflection Radiometer (ASTER) of the Hurghada area, (b) ratio image of band 4 of TM and band 2 of ASTER of the Hurghada area, (c) overlay image of band 3 of TM and band 3N of ASTER of the Hurghada area and (d) principal component (PC) image indicating the temporal changes of an 18-year period (1987–2005).

6.2.3 Image overlay. Image overlay is the simplest way to produce a change detection map from comparison of a single band of data from two dates (Sunar 1998). Moufaddal (2005) added that it is a straightforward way of comparing historical data and provides a qualitative change between two dates. Lu *et al.* (2004) concluded that

image overlay can be implemented by inserting one band from date 1 as red, the same band from date 2 as green and the same band from date 3 as blue, if available.

In this investigation, the change images were produced by inserting the older band in green and the younger one, which is to overlay it, in red according to Howarth and Boasson (1983). Overlay trials of band 3 of TM and band 3N of ASTER highlighted the urban growth and shoreline development (figure 3(c)). The changes in the urban area appeared in a faint green colour and the landfilling along the shoreline in a violet colour.

6.2.4 Multidate PCA. PCA has been proven to be of significant value in the analysis of remotely sensed digital data (Jensen 1986). The transformation of the raw remotely sensed data using PCA can result in principal component (PC) images that are often more interpretable than the original data (Byrne *et al.* 1980). PCA may be used to compress the information content of a number of bands of imagery (e.g. seven thematic mapper bands) into just two or three transformed PC images (Jensen 1986).

In this study, the six non-thermal bands (1, 2, 3, 4, 5 and 7) of TM and ETM+ were gathered in a single file. In addition, six bands of ETM+ and three bands (1, 2 and 3N) of ASTER were gathered in a single file, as well as six bands of TM and three bands of ASTER were gathered in a single file. Then each of the three produced files was subjected to PCA to create a number of PCs. The visual inspection of the PCA colour composites, which are produced from these components, indicated that the composite containing the first three PCs was the most informative and produced more colourful colour composite images than spectral colour composites. Dewidar and Frihy (2003) mentioned that the first three PCs contain more than 95% of the total variance. Therefore, a composite image is integrated from the first three PCs (i.e. PC1 = red, PC2 = green and PC3 = blue) of the file containing temporal change between two dates and highlight clearly the areas of urbanization in brownish yellow colour in the study area (figure 3(d)).

6.2.5 Post-classification comparisons. The post-classification comparisons of derived thematic maps go beyond simple change detection and attempt to quantify the different types of change (Shalaby and Tateishi 2007). Computer-assisted classification of remote sensing data can be partitioned into two general approaches: supervised and unsupervised. The supervised one only will be discussed here. Lillesand and Kiefer (2000) summarized that the typical supervised classification has three basic steps: (1) the training stage, (2) the classification stage and (3) the output stage.

Depending on the prior knowledge of the study area, which was gathered through a combination of reference data and ground data collected during fieldwork, 10 predefined cover classes were designed as basement rocks, Miocene rocks, sabkha deposits (salt marshes), alluvial deposits, wadi (dry valley) deposits, green land (mangroves, farmlands and golf courses), urban (built-up, tourist activities, roads, airport runways), reef flat, coral reef and seawater. Three training classes files were generated, one file for each date, where the aforementioned four change detection methods were helpful to detect areas of change. The distribution of the sites of these training classes throughout the image increases the chance that the training data will be representative of all variations in the cover classes presented in the image. Foody *et al.* (2006) found that there is a positive relationship between the size of the training set and the accuracy of the classification. In addition, the spectral separability of the training class

pairs was examined by computing the Jeffries–Matusita (J–M) distance. The values of the J–M distance range from 0.0 to 2.0, where values greater than 1.9 indicate that training class pairs have good separability (Richards and Jia 1999). The spectral separability between training class pairs of the images of years 1987, 2000 and 2005 ranged between 1.2 and 2.0.

The three images of years 1987, 2000 and 2005 were subjected to the maximum likelihood classifier independently using the training classes of each date. The early attempts of the classification process of each image showed that a little confusion occurs between some spectrally similar classes, for example, confusions between urban area and other classes. Therefore, it was hypothesized that subdividing each multivariate dataset into two sections (land and water) and performing a maximum likelihood classifier on each section independently would resolve a major part of the confusion and would improve the accuracy of the change maps. The two new sections were reproduced by employing a binary mask to the original multivariate datasets. The first section highlights the mainland area and islands and was given by masking the water area. The second highlights the water area only and was given by masking the mainland and offshore islands. Later, direct supervised classification using the maximum likelihood classifier was performed independently on both sections and successful classes from each attempt were edited and ultimately gathered by the GIS function in three collective change maps of the 1987 date, the 2000 date and the 2005 date, with satisfactory accuracy.

6.3 Post-classification procedures

A post-classification treatment was performed using the 3×3 majority filter to eliminate the isolated pixels in the three produced maps (Jensen *et al.* 1993). The classified maps were compared with the source images and some minor isolated pixels were edited on screen, which does not affect the final accuracy of the resulted maps. Then, accurate LULC maps of years 1987 (figure 4(a)), 2000 (figure 4(b)) and 2005 (figure 4(c)) were produced. In addition, an image of urban and built-up land was extracted from these LULC maps (figure 4(d)).

The accuracy assessment was performed independently for the produced classification maps of the years 1987, 2000 and 2005 with the aid of ancillary data and visual interpretation. An accuracy assessment process was carried out using a stratified random sampling design. This sampling design can be appropriate if the sample size is large enough to ensure that all classes are adequately represented (Foody 2002). Therefore, a proportional number of test points were randomly selected from each classification map to assess classification accuracies. Then, a confusion matrix was produced, from which the overall accuracy, user's and producer's accuracies and kappa coefficient were computed for each LULC map (table 1(a)–(c)).

For the 1987 LULC map, a total of 4599 pixels were randomly selected, which were then checked with reference to topographic maps produced in 1989 at a scale of 1:50 000 and the geologic map produced in 1987 at a scale of 1:250 000. The results revealed an overall accuracy of 87.8% and a kappa coefficient of 0.85 (table 1(a)). In terms of producer's accuracy, all classes except alluvial deposits were over 73.3%, while in terms of user's accuracy, all classes were over 77.7%. For the 2000 LULC map, a total of 5010 pixels were randomly selected, which were checked with the land use map of the Hurghada area produced in 1999 at a scale of 1:15 000 and fieldwork data. The result showed an overall accuracy of 88.9% and a kappa coefficient of 0.86 (table 1(b)). The alluvial deposits had the lowest value of producer's accuracy, while the other

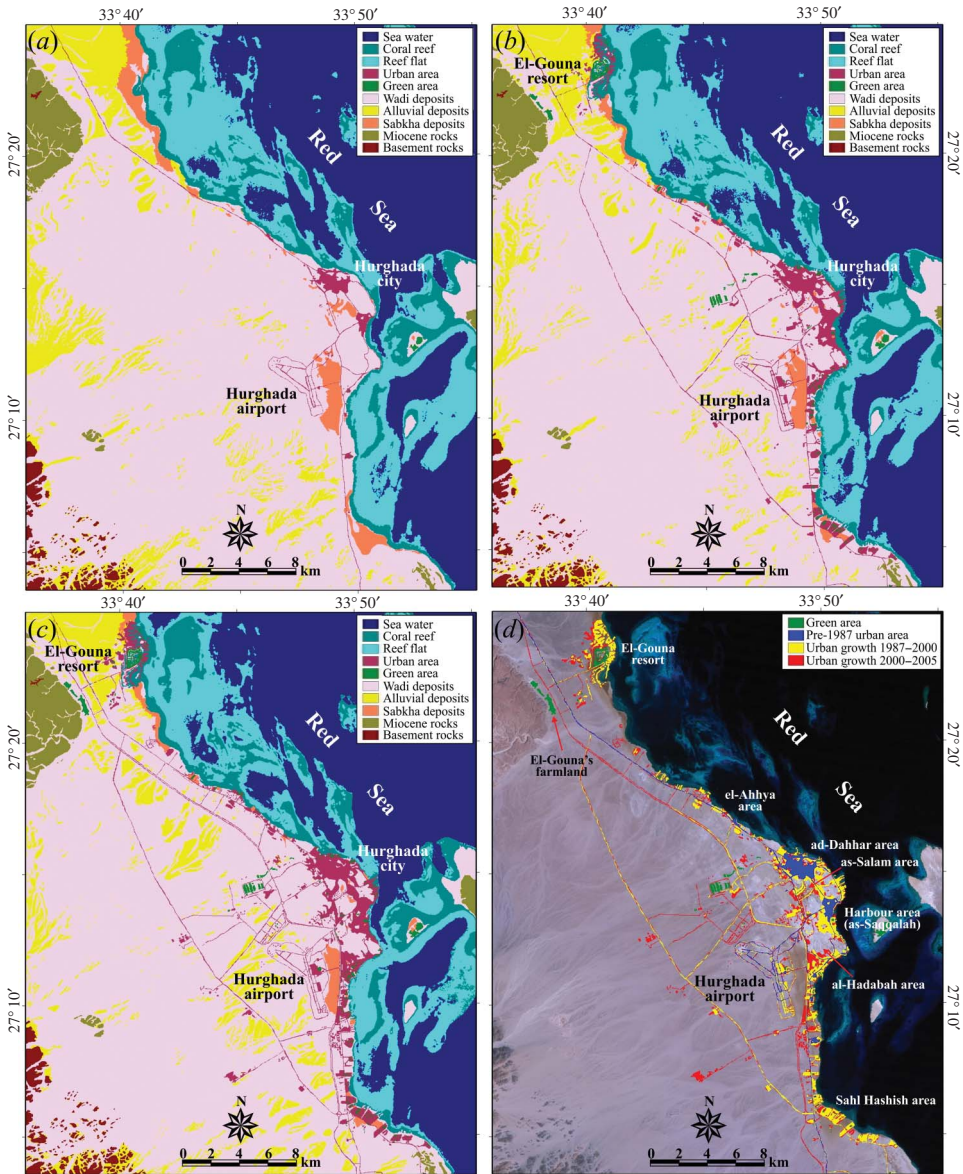


Figure 4. Land use/land cover maps of the Hurghada area of years (a) 1987, (b) 2000 and (c) 2005, and (d) change detection map indicating the urban expansion and its spatial patterns in the Hurghada area through an 18-year period (1987–2005).

classes exhibited accuracies over 82.6%. In terms of user's accuracy, all classes were over 80.9%. For the 2005 LULC map, a total of 5446 pixels were randomly selected, which were validated by the geologic map produced in 2005 at a scale of 1:250 000 and field surveying, which was carried out during August 2006 with the assistance of the GPS (Magellan 530). Table 1(c) shows the overall accuracy of 92.0% and the kappa coefficient of 0.89. All classes had producer's accuracies of over 75.6%, except the alluvial deposits, while in terms of user's accuracy, all classes are over 82.1%.

Table 1. Confusion matrix of land use/land cover maps derived from the satellite data.

		Reference data											Total	CR	RF	SW	BR	MR	SD	AD	WD	GL	UR	PA (%)	UA (%)
		UR	GL	WD	AD	SD	MR	BR	SW	RF	CR	Total	PA (%)	UA (%)											
<i>(a) 1987 (TM)*</i>		199	0	0	10	0	0	0	0	0	0	209	92.1	95.2											
	UR	1	11	0	0	0	0	0	0	0	0	12	73.3	91.7											
	GL	16	4	1372	304	26	43	1	0	0	0	1766	91.9	77.7											
	WD	0	0	120	623	0	0	26	0	0	0	769	66.5	81.0											
	AD	0	0	0	0	194	0	0	0	0	0	194	88.2	100.0											
	SD	0	0	0	0	0	525	0	0	0	0	525	92.4	100.0											
	MR	0	0	0	0	0	0	125	0	0	0	125	82.2	100.0											
	BR	0	0	0	0	0	0	0	644	0	0	644	100.0	100.0											
	SW	0	0	0	0	0	0	0	0	115	7	122	97.5	94.3											
	RF	0	0	0	0	0	0	0	0	3	230	233	97.1	98.7											
	CR	0	0	0	0	0	0	0	0	118	237	4599													
	Total	216	15	1492	937	220	568	152	644	118	237	4599													
<i>(b) 2000 (ETM+)†</i>		277	0	10	0	0	0	0	0	0	0	287	91.1	96.5											
	UR	13	67	0	0	0	0	0	0	0	0	80	95.7	83.8											
	GL	11	0	1818	275	20	120	1	0	0	0	2245	96.3	80.9											
	WD	0	0	60	350	1	0	2	0	0	0	413	56.0	84.8											
	AD	3	3	0	0	126	0	0	0	0	0	132	85.7	95.5											
	SD	0	0	0	0	0	569	0	0	0	0	569	82.6	100.0											
	MR	0	0	0	0	0	0	186	0	0	0	186	98.4	100.0											
	BR	0	0	0	0	0	0	0	676	0	0	676	97.9	100.0											
	SW	0	0	0	0	0	0	0	0	142	19	175	98.6	81.1											
	RF	0	0	0	0	0	0	0	0	2	245	247	92.8	99.2											
	CR	0	0	0	0	0	0	0	0	0	264	5010													
	Total	304	70	1888	625	147	689	189	690	144	264	5010													
<i>(c) 2005 (ASTER)‡</i>		294	4	9	0	3	0	0	0	0	0	310	91.9	94.8											
	UR	16	78	0	0	1	0	0	0	0	0	95	91.8	82.1											
	GL	9	2	2040	212	33	40	1	0	0	0	2337	96.7	87.3											
	WD																								

(Continued)

Table 1. (Continued.)

Reference data												
	UR	GL	WD	AD	SD	MR	BR	SW	RF	CR	Total	UA (%)
AD	0	0	61	442	1	0	2	0	0	0	506	67.5
SD	1	1	0	0	118	0	0	0	0	0	120	75.6
MR	0	0	0	0	0	671	0	0	0	0	671	94.1
BR	0	0	0	1	0	2	191	0	0	0	194	98.5
SW	0	0	0	0	0	0	0	695	0	0	695	96.9
RF	0	0	0	0	0	0	0	17	195	6	218	98.5
CR	0	0	0	0	0	0	0	5	3	292	300	97.9
Total	320	85	2110	655	156	713	194	717	198	298	5446	87.4

Notes: UR, urban; GL, green land; WD, wadi deposits; AD, alluvial deposits; SD, sabkha deposits; MR, Miocene rocks; BR, basement rocks; SW, sea water; RF, reef flat; CR, coral reef; PA, producer's accuracy; UA, user's accuracy.

*Overall accuracy = 87.8%, kappa coefficient = 0.85.

†Overall accuracy = 88.9%, kappa coefficient = 0.86.

‡Overall accuracy = 92.0%, kappa coefficient = 0.89.

The overall accuracies of the three produced maps (figure 4(a)–(c)) met the minimum accuracy stipulated by Anderson *et al.* (1976) and Lins and Kleckner (1996). Hence, the obtained accuracies were considered to be sufficiently accurate for use in driving the change detection statistics.

7. Results and discussion

7.1 Land cover change and statistics

Change detection analysis is performed not only to detect changes that have occurred, but also to identify the nature of those changes and to determine the areal extent and spatial pattern of those changes (Macleod and Congalton 1998). Therefore, the main advantage of the post-classification comparison approach is its capability of providing descriptive information on the nature of changes that have occurred (Mundia and Aniya 2005).

From the classification maps generated for the years 1987, 2000 and 2005 (figure 4(a)–(c)), the individual class area and change statistics are summarized in table 2. In addition, the classes, areas and changed areas are graphically presented in figure 5(a) and (b). Attention was paid to the urban and green land classes, because they represent the main objective of this study. The urban/built-up areas covered about 8.00 km² in the year 1987 and were increased to 28.60 km² in the year 2000 with an average rate of 1.60 km² year⁻¹. The area was increased by a further 39.60 km² by the year 2005 with an average rate of 2.20 km² year⁻¹. The Hurghada area was expanded by 31.70 km² over the entire study period from 1987 to 2005, with an average rate of 1.75 km² year⁻¹. On the other hand, the green land expanded from 0.38 km² (in 1987) to 3.63 km² (in 2000) with an average rate of 0.25 km² year⁻¹ and to 4.30 km² (in 2005) with an average rate of 0.14 km² year⁻¹.

The LULC conversions were estimated and indicated that increase in the urban area mainly comes from conversions of wadi deposits, sabkha deposits and alluvial deposits to urban land uses during the 18-year period (1987–2005). Of the 31.70 km² of growth in urban land use from 1987 to 2005, 70.80% was converted from wadi deposits, 16.70% from sabkha deposits, 6.70% from alluvial deposits and 5.80% from reef flat.

The relative change of urban area was determined and the annual urban growth rate (AUGR) was calculated (table 3) according to the formula adopted by Xiao *et al.* (2006):

$$\text{AUGR} = \frac{(A_{n+i} - A_i)}{nA_r}, \quad (1)$$

where A_r is the reference urban area; A_{n+i} and A_i represent the urban area or built-up area at time $n + i$ and i , respectively; and n is the length of the calculating period (in years).

Relatively, the Hurghada urban area increased ~400% from 1987 to 2005, where the greatest increase that occurred from 1987 to 2000 was about 261%. The AUGR was 20% from 1987 to 2000, 27.50% from 2000 to 2005 and 22.20% for the entire period from 1987 to 2005 (table 3).

Table 2. Land use/land cover changes for the Hurghada area as extracted from the satellite data.

Land cover class	LULC-1987		LULC-2000		LULC-2005		Area changed (km ²)			
	Area (km ²)	%	Area (km ²)	%	Area (km ²)	%	1987-2000	2000-2005	1987-2005	
Urban	07.93	00.63	28.65	02.29	39.60	03.16	20.72	10.95	31.67	
Green land	00.38	00.03	03.63	00.93	04.30	00.34	03.25	00.67	03.92	
Wadi deposits	591.9	47.26	598.61	47.75	574.80	45.89	06.71	-23.81	-17.08	
Alluvial deposits	91.93	07.34	74.42	05.97	86.76	06.93	-17.61	12.37	-05.15	
Sabkha deposits	21.46	01.71	11.53	00.93	08.55	00.68	-09.95	-02.98	-12.91	
Miocene rocks	24.95	01.99	24.52	01.95	26.18	02.09	-00.46	01.76	01.23	
Basement rocks	11.62	00.93	11.73	00.94	12.46	00.99	00.11	00.76	00.84	
Sea water	305.81	24.41	310.07	24.74	325.41	25.98	04.26	15.37	19.60	
Reef flat	59.94	04.79	59.00	04.71	63.11	05.04	-00.94	04.11	03.17	
Coral reef	137.53	10.97	131.44	10.49	112.24	08.96	-06.09	-19.20	-25.29	
Total	1253.5	100.0	1253.5	100.0	1253.5	100.0	00.00	00.00	00.00	

Note: LULC, land use/land cover.

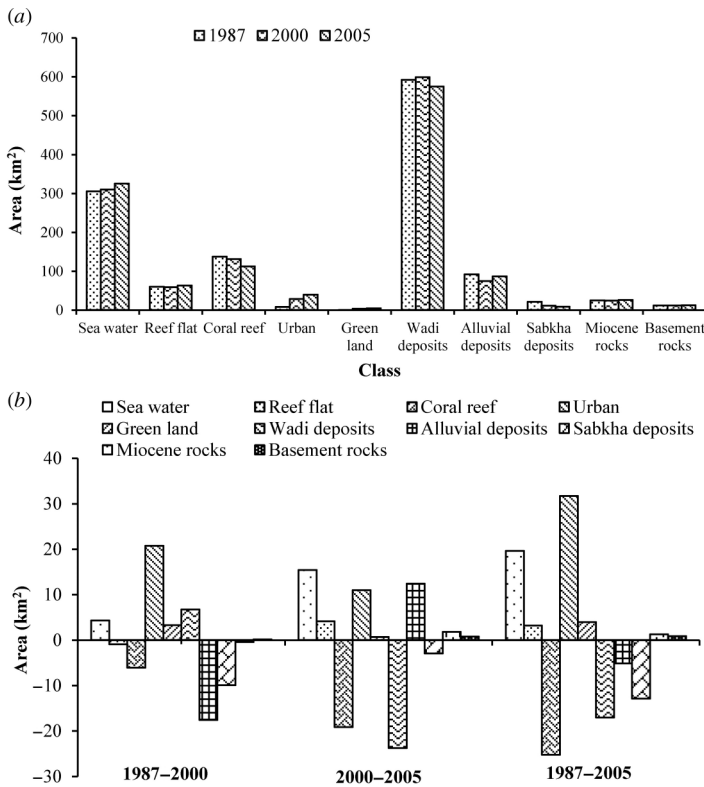


Figure 5. (a) The land use areas of the 10 classes derived from the classified maps. Note that each hatching represents a class in the studied 3 years (1987, 2000 and 2005) and (b) the land use change areas in the studied three epoch time series (1987–2000, 2000–2005 and 1987–2005).

Table 3. Relative change and annual urban growth rate of the Hurghada area (1987–2005).

Period	1987–2000 (%)	2000–2005 (%)	1987–2005 (%)
Relative change of urban area	261	138	400
Annual urban growth rate	20.0	27.6	22.2

7.2 The spatial patterns of urban expansion

In order to analyse the patterns and locations of urban land change, an image of urban and built-up land was extracted from each LULC map (figure 4(a)–(c)). The extracted images were then overlaid onto the Landsat 5 TM (1987) image to obtain an urban land change (expansion) image (figure 4(d)). From this urban expansion image, it can be concluded that the urban region is largely broadened. The growth of the Hurghada city has not taken place evenly in all directions but has occurred much faster in certain directions. The Red Sea represents a natural constraint for expansion of the city in the eastward direction. The city has tremendously expanded in the west and southwest directions and parallel to the Red Sea coast (figure 4(d)).

Hurghada in 1987 was comprised essentially of two areas: ad-Dahhar area (old city) and the Harbour area (as-Saqqalah) (figure 4(d)); from these two nuclei the city began

to expand. In the first stage (1987–2000), the expansion model (Wilson *et al.* 2003) or urban fringe development (Heimlich and Anderson 2001) was the dominant model, which was characterized by a non-developed pixel being converted to developed and surrounded by no more than 40% of existing developed pixels (Wilson *et al.* 2003). The city growth has occurred around the periphery of the ad-Dahhar and Harbour areas (figure 4(d)) and along the main transportation routes (e.g. an-Nasr, as-Salam and al-Kurnish roads), which connected the two main sectors of the city, resulting in a nearly elongate city shape.

In the same time, according to the dramatic increase of the tourist and recreational activities during the 1990s in the Hurghada area, the urban area expanded in a linear fashion parallel to the Red Sea coast from the northernmost area (El-Gouna resort) until the southernmost area (Sahl Hashish area) (figure 4(d)). It is obvious how the pristine coastline of Hurghada area in 1987 transformed into a concrete strip of tourist hotels and recreational facilities during the 18-year period until 2005.

In the second stage (2000–2005), as a result of the improvement of the infrastructures in Hurghada city, the infill growth was developed. The presence of facilities such as sewers, water and roads assisted in developing areas of as-Salam and al-Hadabah within the city, and some of the inner urban areas. In addition, El-Gouna resort, El-Gouna's farmlands, the new community of al-Ahhya area, Hurghada airport, the sewage station and recycling factory are obvious examples of outlying or isolated growth (Wilson *et al.* 2003) or development beyond the urban fringe (Heimlich and Anderson 2001) (figure 4(d)).

7.3 Driving forces for the urban expansion

The urbanization rate of the Hurghada area has been rapid compared with other Egyptian areas. Therefore, the discussion of the factors that influenced this urban expansion is very useful. Generally, urban expansion and subsequent landscape changes are driven by geographical and socio-economical factors, such as population growth, national policy and economic development or a combination of these factors (Ji *et al.* 2001, Cheng and Masser 2003, Xiao *et al.* 2006). Some of these factors can be discussed here as follows.

7.3.1 Urban population growth. Population growth is one of the major dominant driving urbanization processes (Xiao *et al.* 2006). To examine and evaluate the relationship between the population growth and urban expansion of the Hurghada area, the demographic data and urban development areas from 1980 to 2020 were surveyed and are presented in table 4 and figure 6. In the monitoring period of this study from 1987 to 2005, the urban area has increased from ~8 to 39.6 km², with a corresponding increase in population from 23 010 to 82 050 (table 4). This reveals that the population of the Hurghada area has grown from 1987 to 2005 by about 256.5%, while the amount of urban development has extended by about 400%, that is, more than 1.5 times the rate of population growth. This implies that the rate of urban development in the Hurghada area has outstripped the rate of population growth. This can be explained by uncontrolled extension of tourist activities together with the poor planning in the area that led to the use of land for urbanization at a faster rate.

Figure 6 shows that the increase in urban area correlates strongly with population growth in a linear form, with a high coefficient of determination (R^2) of 0.97. This linear regression between urban and population growth offered a more robust prediction

Table 4. Population and urban area of Hurghada city from 1980 to 2020.

Year	Population*	Percentage growth in population (%)	Urban area (km ²)	Percentage increase in urban area (%)
1980	12 472	—	03.1‡	—
1987	23 010	84.5	07.9	154.8
1990	25 458	10.6	08.5‡	07.6
2000	64 363	152.8	28.7	273.6
2005	82 050	27.5	39.6	37.9
2010	100 000†	21.9	48.4§	22.2
2015	133 000†	33.0	57.1§	17.9
2020	174 000†	30.8	66.0§	15.6

Notes: *Population after CAPMAS (1980–2005).

†Expected population after GOPP (1993).

‡Areas after El-Bana (2002).

§Areas calculated according to the average growth rate of this study.

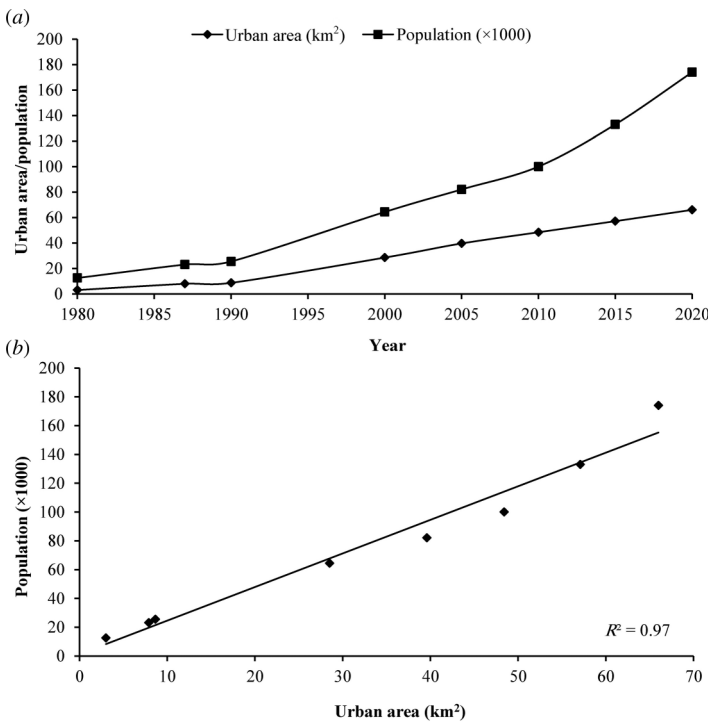


Figure 6. (a) Graphical representation of the growth of population and urban sites of Hurghada area from 1980 to 2020 and (b) positive linear correlation between population growth and urban expansion for Hurghada area.

of urban growth in the Hurghada area, that is, the area is in a constant state of transition. In addition, according to the national policy of the Egyptian authorities, which encourages population shifting to the desert areas in order to overcome the overpopulation problem in the Nile Valley strip, the General Organization for Physical Planning (GOPP) (1993) expected that the population of the Hurghada area will be 174 000 by the year 2020, with the population growth rate of about 112% of what it was in 2005

(table 4). Clearly, this rapid urban population increase is a result of the increasing natural population and migration of people from different areas of Egypt to Hurghada for job opportunities. El-Bana (2002) pointed out that the immigrants to Hurghada area represented about 24% of the population in the year 1986 and about 49% in the year 1996. Comprehensive planning is needed to cope with the increasing demand of this population pressure and to manage the available resources efficiently.

7.3.2 Economic development. The coastlines along the Red Sea and the Gulf of Aqaba are the focus points for one of the fastest growing tourism economies in the world (Tourism Development Authority (TDA) 1998). This coastal tourism plays a major role in Egyptian economic activities. Already, coastal-oriented tourism has created significant communities at Sharm el Sheikh and Hurghada and the two cities have grown to an extent that their beaches are occupied by several kilometres of tourist and recreational activities. Moufaddal (2005) mentioned that resort development and tourism activities along the coastline between Hurghada and Safaga has expanded rapidly in the last 20 years. Undoubtedly, this growth in tourism activities will increase both the urban area and population in the study area. On the other hand, the improvement of the infrastructure and road network also played an important role in promoting the urban development. The road network in Hurghada area has increased from 106 km in the year 1987 to 251 km in the year 2000 and to 262 km in the year 2005.

7.3.3 Topographical and geological factors. Topography forms an important determinant for site suitability and plays a role in the urban development directions. The DEM and slope map of Hurghada city (figure 7(a)) were constructed to study the effect of the physical setting on urban development in the Hurghada area. In the vicinity of Hurghada city are small Tertiary faulted blocks, such as the northern and southern plateaus, which generally orient NNW and NW, respectively (figure 7(b)). Most of the city region has generally a gentle slope (0° – 6°), except around the elevated plateaus, where the slope reaches about 45° . The urban expansion of Hurghada city tended to follow flat areas, especially in the centre (around ad-Dahhar area) and in the south (around the Harbour area) of the city (figure 7(a) and (b)). This expansion was constrained by the existence of the elevated plateaus (e.g. northern plateau) in the city region. It is obvious that these hilly terrains significantly oriented the urban expansion of the city in certain directions. In addition, the presence of many sharms and marinas along the coastline played an important role in the linear expansion of Hurghada and El-Gouna. The wide coastal plain in the Hurghada region will help the city to expand westwardly in the future.

8. Coastline change due to urban coastal development

The urban coastal development commonly creates a number of changes and problems in the nearby shoreline due to the construction of harbours and tourist activities. From the aforementioned discussion, it can be concluded that the coastline of the Hurghada area has experienced considerable environmental stress from tourist and residential activities and, unfortunately, these activities were developed rapidly, uncontrolled and environmentally not planned.

Dredging and land infilling of the backshore and fringing reef areas are considered to be one of the most devastating activities on the coastal environment at Hurghada area (Moufaddal 2005). Frihy *et al.* (1996) pointed out that large amounts of fill

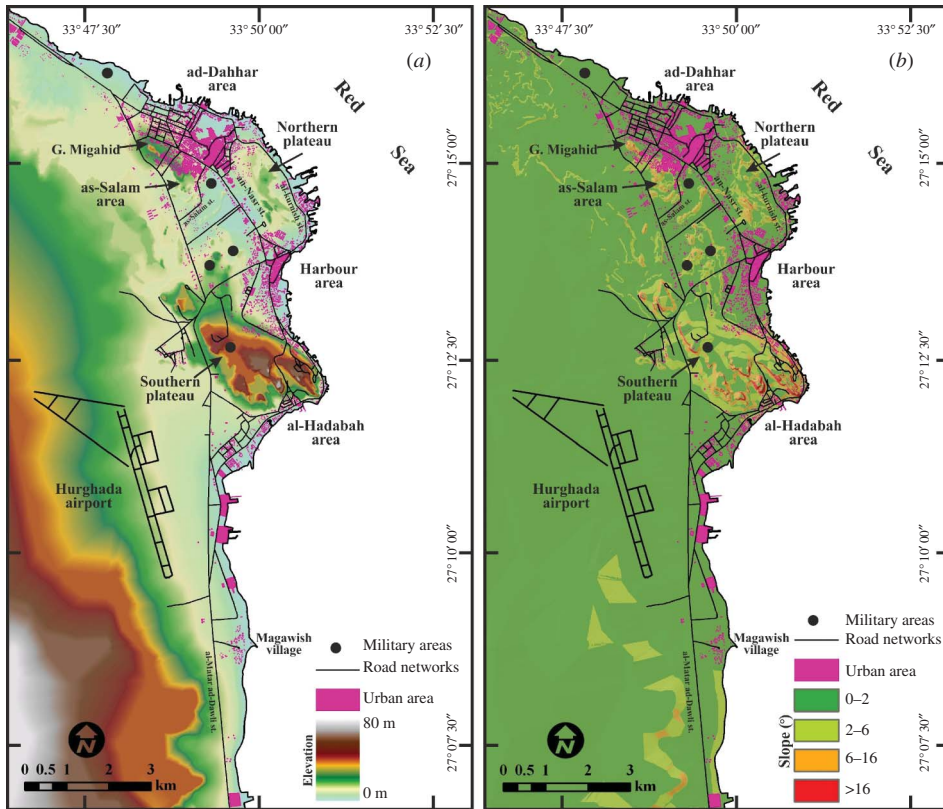


Figure 7. (a) Digital elevation model (DEM) and (b) slope map of Hurghada city region.

material have been dumped in front most of the tourist activities when constructing solid marinas or gaining a new seaward land. In addition, the excavation processes in the coral reef flat for creating artificial swimming pools or water pathways led to great damage (Dewidar 2002). These conditions led Wilson (1998) to say that the situation in the northwestern part of the Red Sea coast becomes especially worrisome, where the main environmental threats are coming from the booming of the tourism industry and urban coastal development projects.

In this study, the processing of satellite data by image differencing and image overlay techniques (figure 3(a) and (d)) shows the extra land which has been added to the sea and how the landfill/sedimentation operations have changed the morphology of the shoreline. The estimated landfilling along the coastline from El-Gouna resort at the north of Hurghada to Sahl Hashish area at the south was 4.5 km² over the period of study (1987–2005). The greatest increase that occurred from 1987 to 2000 was about 3.0 km² and the new land gained from 2000 to 2005 was 1.5 km². This means that most of the fringing reefs in the coastal zone have been replaced by a layer of imported sand and other solid dumping materials (Moufaddal 2005). Vanderstraete *et al.* (2006) mentioned that a clear distinction between the natural and anthropogenic changes in the coastline could not be made, but they attributed most of these changes to the urban coastal development.

It is important to mention that Dewidar (2002) estimated the landfilling in the vicinity of Hurghada as 2.0 km² between 1984 and 1997 (table 5). Moufaddal (2005) calculated

Table 5. Available published estimates of the coastline changes in Hurghada region.

Study	Interval	Period (years)	Remotely sensed data used	Coastline changes (km ²)		
				Landfill	Dredging	Total
Dewidar (2002)	1984–1997	13	TM	2.0	–	2.0
Moufaddal (2005)	1984–2000	16	TM, ETM+	3.6	2.9	6.5
Vanderstraete <i>et al.</i> (2006)	1987–2000	13	TM, ETM+	4.0	2.0	6.0
This study	1987–2005	18	TM, ETM+, ASTER	4.5	–	4.5

the total area subjected to landfilling and dredging in the coastal strip from north of Hurghada to south of Safaga between 1984 and 2000 as 6.5 km². Of this area, 3.6 km² was used as landfill and 2.9 km² was used as the dredging area. Recently, Vanderstraete *et al.* (2006) determined the areal extent of the coastline changes in the Hurghada area between 1987 and 2000 as 6.0 km². Of these changes, 4.0 km² was used as landfill and 2.0 km² was used as the dredging area (table 5). The differences between our results and the above results are largely attributed to difference in methodology and the time period of study, as well as the extent of the studied areas along the Red Sea coast. Importantly, far from these different estimates, the conclusion remained that the dramatic urban expansion of Hurghada area led to major changes in the coastline zone.

9. The future directions of Hurghada urban expansion

From the above expansion analysis and the forecasts that are currently available, it seems that the urban expansion of Hurghada in the next years is an inevitable process. Therefore, discussion on the amount, direction and location of this future expansion is extremely valuable to urban planners, who can use this information to monitor the impacts of this growth and to evaluate and modify the existing urban policies and develop appropriate responses or strategies.

The future directions of Hurghada expansion are governed by some natural and artificial constraints which compelled the physical form of the city. The natural constraints include the Red Sea shoreline, the drainage network and topographical features. The Red Sea shoreline restricts the city to eastward expansion, although it can be a positive factor for the coastal urban growth. Hurghada city and its vicinity were constructed at the mouths of some wadis (e.g. W. al-Faliq al-War and W. al-Faliq al-Sahl), which emanate from the basement rocks at the west. The courses of the wadis must be left clean to avoid damage from flash flooding, which occurs from time to time.

The artificial constraints include Hurghada airport and military areas. Hurghada airport is considered to be a major constraint to urban growth of Hurghada in the southwestward direction (figure 7). Its safety zone and the noise corridor of the aircraft will be major problems in the future (Arafat *et al.* 2007). On the other hand, the military areas within Hurghada city represent a major constraint to inner urban growth (figure 7). These areas represent about 35% of the total area of the city (El-Bana 2002).

Indeed, the present unplanned Hurghada and its uncontrolled expansion during the span of time indicate that deliberate planning is largely lacking and the general urban principles encoded in various laws and government regulations have not been adhered

to or enforced. Therefore, comprehensive planning is needed to anticipate and estimate the future city growth.

GOPP (1993) presented a detailed report on Hurghada, which included two scenarios for the future land use planning of the Hurghada area until 2020 (figure 8).

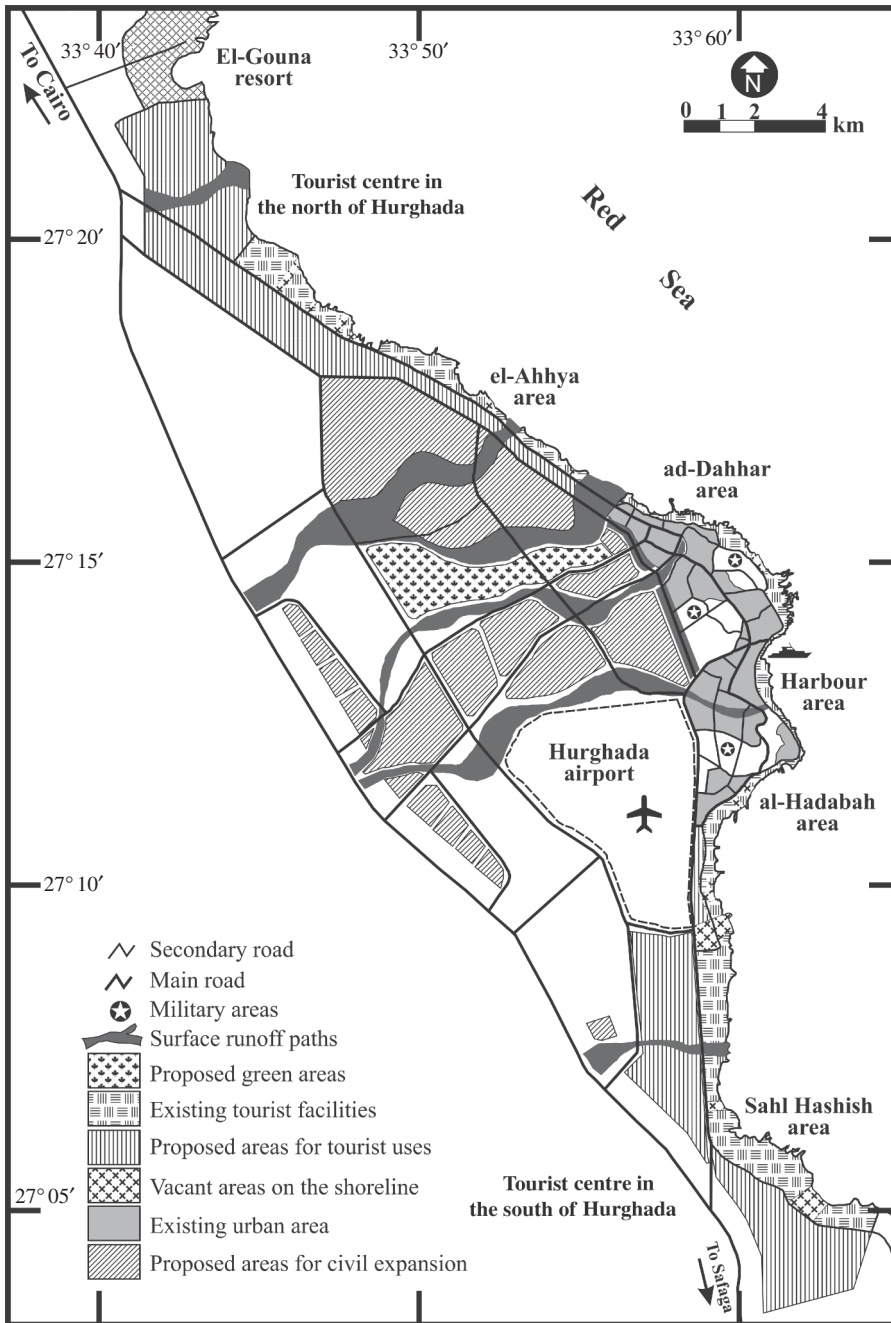


Figure 8. Proposed land use planning for the Hurghada area until 2020 (simplified after General Organization for Physical Planning (GOPP) (1993) and Red Sea Governorate (RSG) (2000)).

Then, this land use planning was revised by RSG (2000). The report expected that the Hurghada area will be about 57 km² and its population will be more than 174 000 by the year 2020. But in accordance with the AUGR, which is estimated in this study (1.75 km² year⁻¹), the Hurghada area will be around 66 km² in the year 2020. Consequently, the local authorities are facing numerous challenges such as population pressure and inadequate infrastructure and services. Therefore, regular monitoring and up-to-date information about land uses form the basis for better planning and effective spatial organization of urban activities for the future development of the Hurghada area.

10. Conclusions and recommendations

This study is considered to be an attempt to detect and evaluate urban land use change in the Hurghada area by applying GIS and remote-sensing techniques. Geomorphological, geological and structural characteristics are considered to be important factors that have influenced the site suitability for urban expansion. The integration of demographic data and the results of change detection techniques showed that the Hurghada area has changed significantly. The urban area has increased 400% from 1987 to 2005, with the corresponding growth of population more than 256.5%. In addition, it is noted that tourist activities, population growth and city location were the principal factors driving the development of the urban area. Sadly, the rapid growth of the Hurghada area has been accompanied by landfilling processes, which are considered to be a major negative activity in the coastal zone, where 4.5 km² of sediments have been added to the sea, significantly changing the morphology of the shoreline and negatively affecting the ecosystem.

Urban fringe development and linear growth models are the dominant change pattern over the period from 1987 to 2000, whereas the infill or inner urban growth and isolated growth models are the dominant change pattern over the period from 2000 to 2005. This study emphasized that spatial information (i.e. GIS) and remotely sensed data are particularly helpful in providing time-series information on urban landscape evaluation and this, in turn, provide interesting supports for decision-making for future planning and monitoring plans.

It is clear that the haphazard urban development in Hurghada area is the responsibility of the local authorities, urban planners and managers. Therefore, they are a part of both the problem and the solution. This study offers some recommendations to be used as guidelines in the future planning for the urban expansion of Hurghada area as follows.

- Accurate risk assessment maps for sites vulnerable to flash flooding and precautionary measures should be made.
- Adequate subsurface investigation and geotechnical studies of the Miocene evaporites unit are needed to assess the potential site suitability.
- Short-term and long-term planning are needed because they play an important role in guiding appropriate development to the right place and in preventing development which is not acceptable.
- Monitoring programmes for the urban area and shoreline changes must be adopted by the relevant authorities.
- Preventing all shapes of landfill and dredging processes along the shoreline and enforcement of the environmental laws and regulations.
- Careful planning for expansion over the faulted blocks and serious assessment of the earthquake activities should be made.

- Reshaping the military areas within the city environs or relocating them outside the city to encourage the inner urban expansion and to increase the density in the centre. These areas already have the infrastructure facilities.

Acknowledgements

The authors thank the State Scholarship Foundation (IKY), Greece, for supporting this work and for providing a PhD scholarship to the first author. The authors especially thank Prof. M. Abd El-Wahed and Mr H. Abdel Hameed (Tanta University, Egypt) for helping the first author in the fieldwork. The authors also thank the two anonymous reviewers for their valuable comments and suggestions.

References

- ABRAMS, M. and HOOK, S., 1998, *ASTER User Handbook, Version 1* (Pasadena, CA: NASA Jet Propulsion Laboratory).
- ALBERTI, M., WEEKS, R. and COE, S., 2004, Urban land cover change analysis in central puget sound. *Photogrammetric Engineering and Remote Sensing*, **70**, pp. 1043–1052.
- ANDERSON, J.R., HARDY, E.E., ROACH, J.T. and WITMER, W.E., 1976, A land use and land cover classification system for use with remote sensing data, US Geological Survey professional paper 964 (Washington, DC: United States Government Printing Office), pp. 138–145.
- ARAFAT, M., OSMAN, T. and ABDEL-LATIF, I., 2007, Noise assessment and mitigation schemes for Hurghada airport. *Applied Acoustics*, **68**, pp. 1373–1385.
- BARNESLEY, M.J. and BARR, S.J., 1996, Inferring urban land use from satellite sensor images using kernel-based spatial reclassification. *Photogrammetric Engineering and Remote Sensing*, **62**, pp. 949–958.
- BARREDO, J., KASANKO, M., MCCORMICK, M. and LAVALLE, C., 2003, Modeling dynamic spatial processes: simulation of urban future scenarios through cellular automata. *Landscape and Urban Planning*, **64**, pp. 145–160.
- BATTY, M. and HOWES, D., 2001, Predicting temporal patterns in urban development from remote imagery. In *Remote Sensing and Urban Analysis*, J.P. Donnay, M.J. Barnesley and P.A. Longley (Eds.), pp. 185–204 (London: Taylor & Francis).
- BOUNFOUR, A. and LAMBIN, E., 1999, How valuable is remotely sensed information? The case of tropical deforestation modeling. *Space Policy*, **15**, pp. 149–158.
- BYRNE, G.F., CRAPPER, P.F. and MAYO, K.K., 1980, Monitoring land-cover change by principal component analysis of multitemporal Landsat data. *Remote Sensing of Environment*, **10**, pp. 175–184.
- CENTRAL AGENCY FOR PUBLIC MOBILIZATION AND STATISTICS (CAPMAS), 1980–2006, Official censuses – for different years (1980–2006) – of Population, Housing and Buildings, Cairo.
- CHANDER, G., HELDER, D., MARKHAM, B., DEWALD, J., KAITA, E., THOME, K., MICIJEVIC, E. and RUGGLES, T., 2004, Landsat-5 TM reflective-band absolute radiometric calibration. *IEEE Transactions on Geoscience and Remote Sensing*, **42**, pp. 2747–2760.
- CHANDER, G., MARKHAM, B. and BARSIS, J., 2007, Revised Landsat-5 thematic mapper radiometric calibration. *IEEE Geoscience and Remote Sensing Letters*, **4**, pp. 490–494.
- CHAVEZ, P.S., 1996, Image-based atmospheric correction-revisited and improved. *Photogrammetric Engineering and Remote Sensing*, **62**, pp. 1025–1036.
- CHEN, X., 2002, Using remote sensing and GIS to analyze land cover change and its impact on regional sustainable development. *International Journal of Remote Sensing*, **22**, pp. 1–18.
- CHEN, X., VIERLING, L. and DEERING, D., 2005, A simple and effective radiometric correction method to improve landscape change detection across sensors and across time. *Remote Sensing of Environment*, **98**, pp. 63–79.

- CHENG, J. and MASSER, I., 2003, Urban growth pattern modeling: a case study of Wuhan city, PR China. *Landscape and Urban Planning*, **62**, pp. 199–217.
- COLLETA, B., LEQUELLEC, P., LETOUZEY, J. and MORETTI, I., 1988, Longitudinal evolution of the Suez Rift structure (Egypt). *Tectonophysics*, **153**, pp. 221–233.
- COPPIN, P.R. and BAUER, M.E., 1996, Digital change detection in forest ecosystems with remote sensing imagery. *Remote Sensing of Environment*, **13**, pp. 207–234.
- DALE, V., SOUTHWORTH, F., O'NEILL, R., ROSEN, A. and FROLIN, R., 1993, Simulating spatial patterns of land use changes in Rondonia, Brazil. *Lectures on Mathematics in the Life Sciences*, **23**, pp. 29–55.
- DARWISH, M. and EL-AZABI, M., 1993, Contributions to the Miocene sequences along the western coast of the Gulf of Suez, Egypt. *Egyptian Journal of Geology*, **37**, pp. 21–47.
- DEWIDAR, K.H.M., 2002, Landfill detection in Hurghada, North Red Sea, Egypt, using thematic mapper images. *International Journal of Remote Sensing*, **23**, pp. 939–948.
- DEWIDAR, K.H.M. and FRIHY, O.E., 2003, Thematic mapper analysis to identify geomorphologic and sediment texture of El Tineh plain, north-western coast of Sinai, Egypt. *International Journal of Remote Sensing*, **24**, pp. 2377–2385.
- DU, Y., TEILLET, P.M. and CIHLAR, J., 2002, Radiometric normalization of multitemporal high-resolution satellite images with quality control for land cover change detection. *Remote Sensing of Environment*, **82**, pp. 123–134.
- EGYPTIAN GEOLOGICAL SURVEY AND MINING AUTHORITY (EGSMA), 2005, Geologic map of Hurghada quadrangle, Egypt, Scale 1:250 000.
- EL-BANA, A.F., 2002, The urban change in Hurghada city in the quartet of the 20th century. MSc thesis, Tanta University, Tanta, Egypt, 314 p.
- ENVIRONMENT FOR VISUALIZING IMAGES (ENVI), 2004, *ENVI User's Guide. Software Package V. 4.5*, 1128 pp. (Boulder, CO: Research Systems Inc.).
- FOODY, G.M., 2002, Status of land cover classification accuracy assessment. *Remote Sensing of Environment*, **80**, pp. 185–201.
- FOODY, G.M., MATHUR, A., SANCHEZ-HERNANDEZ, C. and BOYD, D., 2006, Training set size requirements for the classification of a specific class. *Remote Sensing of Environment*, **104**, pp. 1–14.
- FRIHY, O., FANOS, A., KHAFAGY, A. and ABU AESHA, K., 1996, Human impacts on the coastal zone of Hurghada, northern Red Sea, Egypt. *Geo-Marine Letters*, **16**, pp. 324–329.
- GENERAL ORGANIZATION FOR PHYSICAL PLANNING (GOPP), 1993, *General Land Use Planning of Hurghada Area Until the Year 2020* (Cairo: Ministry of Housing, Utilities, and Urban Development).
- GREY, W.M., LUCKMAN, A.J. and HOLLAND, D., 2003, Mapping urban change in the UK using satellite radar interferometry. *Remote Sensing of Environment*, **87**, pp. 16–22.
- HE, C., OKADA, N., ZHANG, Q., SHI, P. and ZHANG, J., 2006, Modeling urban expansion scenarios by coupling cellular automata model and system dynamic model in Beijing, China. *Applied Geography*, **26**, pp. 323–345.
- HEIMLICH, R.E. and ANDERSON, W.D., 2001, *Development at the Urban Fringe and Beyond: Impacts on Agriculture and Rural Land*, ERS Agricultural Economic Report No. 803 (Washington, DC: ERS, US Department of Agriculture) 88 p.
- HEROLD, M., GOLDSTEIN, N. and CLARKE, K., 2003, The spatiotemporal form of urban growth: measurement, analysis and modeling. *Remote Sensing of Environment*, **86**, pp. 286–302.
- HOWARTH, P.J. and BOASSON, E., 1983, Landsat digital enhancements for change detection in urban environments. *Remote Sensing of Environment*, **13**, pp. 149–160.
- HUSSEIN, H., MARZOUK, I., MOUSTAFA, A. and HURUKAWA, N., 2006, Preliminary seismicity and focal mechanisms in the southern Gulf of Suez: August 1994 through December 1997. *Journal of African Earth Sciences*, **45**, pp. 48–60.
- JENSEN, J.R., 1986, *Introductory Digital Image Processing. A Remote Sensing Perspective*, 379 p. (Englewood Cliffs, NJ: Prentice-Hall).

- JENSEN, J.R., COWEN, D.J., ALTHAUSEN, J.D., NARAMALANI, S. and WEATHERBEE, O., 1993, An evaluation of coastwatch change detection protocol in South Carolina. *Photogrammetric Engineering and Remote Sensing*, **59**, pp. 1039–1046.
- JI, C.Y., LIU, Q., SUN, D., WANG, S., LIN, P. and LI, X., 2001, Monitoring urban expansion with remote sensing in China. *International Journal of Remote Sensing*, **22**, pp. 1441–1455.
- KARUGA, J.G., 1993, *Actions Towards a Better Nairobi: Report and Recommendations of the Nairobi City Convention*, July 1993, City Hall, Nairobi.
- IRISH, R.R. 2000, Landsat 7 Science Data Users Handbook, Report 430-15-01-003-0, National Aeronautics and Space Administration, Goddard Space Flight Center, Maryland. Available online at, <http://landsathandbook.gsfc.nasa.gov/> (accessed 30 April 2008).
- LILLESAND, T. and KIEFER, R., 2000, *Remote Sensing and Image Interpretation*, 721 p. (New York: John Wiley & Sons).
- LINS, K.S. and KLECKNER, R.L., 1996, Land cover mapping: an overview and history of the concepts. In *Gap Analysis: A Landscape Approach to Biodiversity Planning*, J.M. Scott, T.H. Tear and F. Davis (Eds.), pp. 57–65 (Bethesda, MD: American Society for Photogrammetry and Remote Sensing).
- LOVELAND, T.R., MERCHANT, J.W., OHEN, D.O. and BROWN, J.F., 1991, Development of a land cover characteristics database for the conterminous US. *Photogrammetric Engineering and Remote Sensing*, **57**, pp. 1453–1463.
- LU, D., MAUSEL, P., BRONDIZIO, E. and MORAN, E., 2002, Assessment of atmospheric correction methods for Landsat TM data applicable to Amazon basin LBA research. *International Journal of Remote Sensing*, **23**, pp. 2651–2671.
- LU, D., MAUSEL, P., BRONDIZIO, E. and MORAN, E., 2004, Change detection techniques. *International Journal of Remote Sensing*, **25**, pp. 2365–2407.
- MACLEOD, R.D. and CONGALTON, R.G., 1998, A quantitative comparison of change detection algorithms for monitoring eelgrass from remotely sensed data. *Photogrammetric Engineering and Remote Sensing*, **64**, pp. 207–216.
- MATHER, P.M., 1999, *Computer Processing of Remotely-Sensed Images*, 2nd ed. (Chichester: John Wiley & Sons).
- MOHAMED, A., 1999, Sedimentological and geochemical studies on recent shallow water sediments, Red Sea, Egypt. PhD thesis, South Valley University, Egypt, 230 p.
- MONTENAT, C., OTT D'ESTEVOU, P., PURSER, B., BUROLLET, P., JARRIGE, J., SPERBER, F., PHILOBBOS, E., PLAZIAT, J.-C., PRAT, P., RICHERT, J., ROUSSEL, N. and THEIRIET, J., 1988, Tectonic and sedimentary evolution of the Gulf of Suez and the northern western Red Sea. *Tectonophysics*, **153**, pp. 166–177.
- MOUFADDAL, W.M., 2005, Use of satellite imagery as environmental impact assessment tool: a case study from the new Egyptian Red Sea coastal zone. *Environmental Monitoring & Assessment*, **107**, pp. 427–452.
- MÜLLER, D. and ZELLER, M., 2002, Land use dynamics in the central highlands of Vietnam: a spatial model combining village survey data with satellite imagery interpretation. *Agricultural Economy*, **27**, pp. 333–354.
- MUNDIA, N. and ANIYA, M., 2005, Analysis of land use/cover changes and urban expansion of Nairobi city using remote sensing and GIS. *International Journal of Remote Sensing*, **26**, pp. 2831–2849.
- OLTHOF, L., POULIOT, D., FERNANDES, R. and LATIFOVIC, R., 2005, Landsat-7 ETM+ radiometric normalization comparison for northern mapping application. *Remote Sensing of Environment*, **95**, pp. 388–398.
- PAOLINI, L., GRINGS, F., SOBRINO, J., MUNOZ, J. and KARSZENBAUM, H., 2006, Radiometric correction effects in Landsat multi-date/multi-sensor change detection studies. *International Journal of Remote Sensing*, **27**, pp. 685–704.
- PATTON, T.L., MOUSTAFA, A.R., NELSON, R. and ABDINE, S.A., 1994, Tectonic evolution and structural setting of the Suez rift. *AAPG Memoir*, **59**, pp. 9–51.
- RED SEA GOVERNORATE (RSG), 2000, *Strategy of Urban and Tourist Development of Hurghada and Upgrading the General Planning of the Year 1993*, Hurghada City Hall, GIS unit, 80 p.

- RICHARDS, J.A., 1993, *Remote Sensing Digital Image Analysis: An Introduction*, 1st ed., 250 pp. (Berlin: Springer).
- RICHARDS, J.A. and JIA, X., 1999, *Remote Sensing Digital Image Analysis – An Introduction*, 3rd ed. (Berlin: Springer).
- ROMERO, H., IHL, M., RIVERA, A., ZALAZAR, P. and AZOCAR, P., 1999, Rapid urban growth, land use changes and air pollution in Santiago, Chili. *Atmospheric Environment*, **33**, pp. 4039–4047.
- SAAD, R., 1999, El-Gouna: a real community. *Al-Ahram Weekly*, 13–19 May, Issue No. 429.
- SAID, R., 1990, *The Geology of Egypt*, 2nd ed., 734 p. (Rotterdam: A. A. Balkema).
- SAID, R., 1999, East of Edfu. *Al-Ahram Weekly*, 18–24 February, Issue No. 417.
- SCHROEDER, T., COHEN, W., SONG, C., CANTY, M. and YANG, Z., 2006, Radiometric correction of multi-temporal Landsat data for characterization of early successional forest patterns in western Oregon. *Remote Sensing of Environment*, **103**, pp. 16–26.
- SHALABY, A. and TATEISHI, R., 2007, Remote sensing and GIS for mapping and monitoring land cover and land-use changes in the northwestern coastal zone of Egypt. *Applied Geography*, **27**, pp. 28–41.
- SINGH, A., 1989, Digital change detection techniques using remotely-sensed data. *International Journal of Remote Sensing*, **10**, pp. 989–1003.
- SONG, C., WOODCOCK, C.E., SETO, K.C., PAX-LENNEY, M. and MACOMBER, S.A., 2001, Classification and change detection using Landsat TM data: When and how to correct atmospheric effects? *Remote Sensing of Environment*, **75**, pp. 230–244.
- STOW, D.A. and CHEN, D.M., 2002, Sensitivity of multitemporal NOAA AVHRR data of an urbanizing region to land-use/land-cover change and misregistration. *Remote Sensing of Environment*, **80**, pp. 297–307.
- SUNAR, F., 1998, An analysis of changes in a multi-date set: a case study in the Ikitelli area, Istanbul, Turkey. *International Journal of Remote Sensing*, **19**, pp. 225–235.
- THOME, K., MARKHAM, B., BARKER, J., SLATER, P. and BIGGAR, S., 1997, Radiometric calibration of Landsat. *Photogrammetric Engineering and Remote Sensing*, **63**, pp. 853–858.
- TOURISM DEVELOPMENT AUTHORITY (TDA), 1998, *Best Practices for Tourism Center Development Along the Red Sea Coast*, 108 p. (Cairo: Ministry of Tourism)
- VANDERSTRAETE, T., GOOSSENS, R. and GHABOUR, T., 2006, The use of multi-temporal Landsat images for the change detection of the coastal zone near Hurghada, Egypt. *International Journal of Remote Sensing*, **27**, pp. 3645–3655.
- WEBER, C. and PUISSANT, A., 2003, Urbanization pressure and modeling of urban growth: example of the Tunis Metropolitan area. *Remote Sensing of Environment*, **86**, pp. 341–352.
- WILSON, E.H., HURD, J.D., CIVCO, D.L., PRISLOE, M.P. and ARNOLD, C., 2003, Development of a geospatial model to quantify, describe and map urban growth. *Remote Sensing of Environment*, **86**, pp. 275–285.
- WILSON, M., 1998, The GEF Egyptian Red Sea Coastal and Marine Resource Management Project. A decade of effort, experience and trade-offs required to achieve marine tourism and conservation goals. In *Proceedings of International Tropical Marine Ecosystems Management Symposium*, 23–26 November 1998, I. Dight, R. Kenchington and J. Baldwin (Eds.), Townsville, Australia, pp. 239–250.
- XIAO, J., SHEN, Y., GE, J., TATEISHI, R., TANG, C., LIANG, Y. and HUANG, Z., 2006, Evaluating urban expansion and land use change in Shijiazhuang, China, by using GIS and remote sensing. *Landscape and Urban Planning*, **75**, pp. 69–80.
- YOUNES, A. and McCLAY, K., 2002, Development of accommodation zones in the Gulf of Suez-Red Sea rift, Egypt. *AAPG Bulletin*, **86**, pp. 1003–1026.
- ZHANG, L., YANG, L., LIN, H. and LIAO, M., 2008, Automatic relative radiometric normalization using iteratively weighted least square regression. *International Journal of Remote Sensing*, **29**, pp. 459–470.